JOURNAL OF COMPUTATIONAL PHYSICS 118, 120–130 (1995)

Convergence to Steady State Solutions of the Euler Equations on Unstructured Grids with Limiters

V. VENKATAKRISHNAN*

Computer Sciences Corporation, M.S. T045-1, NASA Ames Research Center, Moffett Field, California 94035

Received July 23, 1993; revised September 7, 1994

This paper addresses the practical problem of obtaining convergence to steady state solutions of the Euler equations when limiters are used in conjunction with upwind schemes on unstructured grids. The base scheme forms a gradient and limits it by imposing monotonicity conditions in the reconstruction stage. It is shown by analysis in one dimension that such an approach leads to various schemes meeting total-variation-diminishing requirements in one dimension. In multiple dimensions these schemes produce steady-state solutions that are monotone and devoid of oscillations. However, convergence stalls after a few orders of reduction in the residual. A new limiter is introduced that is particularly suited for unstructured grid applications. When reduced to one dimension, it is shown that this limiter satisfies the standard theory. With this limiter, it is shown that converged steady-state solutions can be obtained. However, the solutions are not monotone. There appears to be a conflict between achieving convergence and monotone solutions with the higher order schemes that employ limiters in the framework presented.

1. INTRODUCTION

Impressive progress has been made in the area of upwind schemes for the solution of the compressible Euler and the Navier–Stokes equations in the last decade. In their most popular form, upwind schemes are implemented in two stages:

1. A reconstruction stage which obtains a representation of the solution surface given either pointwise or cell-averaged data. Monotonicity principles are also invoked at this stage to enable discontinuities to be captured without oscillations.

2. The reconstructed variables on either sides of the interfaces between the control volumes are interpreted as initial data for approximate Riemann solvers.

In recent years, many upwind schemes have been extended to unstructured grids for solving the compressible Euler equations. For upwind schemes to work well on unstructured grids it stands to reason that true multi-dimensionality be reflected both in the reconstruction and the Riemann solver stages. While truly multi-dimensional Riemann solvers have been investigated by a number of researchers with varying degrees of success, in this work the grid-aligned one-dimensional approximate Riemann solver of Roe [1] will be used since the issues addressed in this paper are independent of this choice. Some of the upwind schemes in use for unstructured grids are rather formal extensions of one-dimensional models [2, 3] even in the reconstruction stage, without much rigorous theory to support them. However, on relatively uniform triangular grids, many of these schemes seem to produce good resolutions of shocks and other features. Barth and Jespersen [4] introduced a novel upwind scheme for the solution of the Euler equations on unstructured grids. This scheme first performs a linear reconstruction to interpolate data to the control volume faces and then employs an approximate Riemann solver to compute the fluxes. In the reconstruction stage monotonicity principles are enforced to ensure that the reconstructed values be bounded by the values of a cell and its neighbors. To this end, multi-dimensional limiter functions are used. In contrast to the previous efforts, the reconstruction is truly multi-dimensional. Barth and Jespersen were able to compute smooth oscillation-free transonic flow solutions even on highly irregular triangular meshes.

It has long been known that the use of limiters can severely hamper the convergence of upwind Euler and Navier–Stokes codes to steady state. This particularly nagging problem has somewhat limited the use of these codes in production environments. The convergence problems are even more pronounced in the case of limiters that make use of nondifferentiable functions such as the *max* or the *min* functions. The multi-dimensional limiter of [4] is an example of such a limiter. While these limiters have been carefully designed to avoid oscillations, they also inhibit convergence of nonlinear problems to steady state. Convergence problems with such limiters have not been adequately addressed in the literature. For structured grids, Venkatakrishnan [5], among others, has obtained converged steady-state solutions using differentiable limiters. Convergence was achieved by modifying the limiter function, whereby the limiter is effectively turned off in the freestream regions.

* This work was funded under contract NAS 2-12961. Current address of the author is the Institute for Computer Applications in Science and Engineering (ICASE), M.S. 132C, NASA Langley Research Center, Hampton, VA 23681-0001.

0021-9991/95 $6.00

This modification is similar to that used by van Albada *et al.* [6] in a different context viz., the problem of capturing smooth extrema without clipping.

In this paper, the problem of lack of convergence of the base scheme is investigated. The base scheme of [4] is first analyzed in one dimension to serve as a framework for investigating the problem. It is shown that several upwind schemes that obey the monotonicity conditions given by Spekreijse [12] can be derived from the base scheme. A new limiter is devised that is particularly suited for unstructured grid applications and that also satisfies the theory of total-variation-diminishing TVD schemes in one dimension. This limiter is modified in such a manner that the convergence problems with the base scheme are alleviated in two dimensions. While the base scheme fails to converge to steady state for these problems, the modified scheme is shown to converge quite well.

2. THE PROBLEM

In this work, the compressible Euler equations in integral form are solved on unstructured grids, composed of triangles. The governing equations in integral form for a control volume Ω with boundary $\partial\Omega$ read

$$\frac{d}{dt}\int_{\Omega} \mathbf{u}\, dv + \oint_{\partial\Omega} \mathbf{F}(\mathbf{u}, \mathbf{n})\, dS = 0. \tag{1}$$

Here $\mathbf{u}$ is the solution vector comprised of the conservative variables density, the two components of momentum and total energy. The vector $\mathbf{F}(\mathbf{u}, \mathbf{n})$ represents the inviscid flux vector for a surface with normal vector $\mathbf{n}$. The control volumes are nonoverlapping polygons which surround the vertices of the mesh. They form the *dual* of the mesh, which is composed of segments of medians. Associated with each edge of the original mesh is a (segmented) dual edge. The contour integrals in Eq. (1) are replaced by discrete path integrals over these dual edges. The flux $\mathbf{F}(\mathbf{u}, \mathbf{n})$ is replaced by a numerical flux function. The construction of the numerical fluxes is done in two stages:

1. First, a piecewise linear reconstruction of the variables is performed. The variables are then interpolated to the edges of the control volumes. Monotonicity principles are invoked at this stage to eliminate over/undershoots by using limiters.

2. The variables on either side of the control volume edges are interpreted as initial data for Roe's approximate Riemann solver [1].

A Riemann problem is defined by Eq. (1) subject to two constant states as initial data in one dimension. More details on the spatial discretization may be found in [4].

The adverse effects of limiters on convergence are well known. In some instances it is possible to declare convergence by monitoring quantities other than the residual, the lift coefficient for example, even if the residual stalls. However, if convergence acceleration procedures, such as multigrid, are to be used, it is important that the baseline scheme be actually convergent. In this paper the problem of obtaining converged solutions to the Euler equations on unstructured grids is addressed. While in the case of flows with extremely weak shocks it may be possible to obtain solutions without using limiters, for flows with strong shocks limiters are absolutely essential. Barth and Jespersen [4] demonstrated the effectiveness of their multidimensional limiter by computing oscillation-free transonic flow solutions on highly irregular triangular meshes. They do not address the issue of convergence in their paper, however.

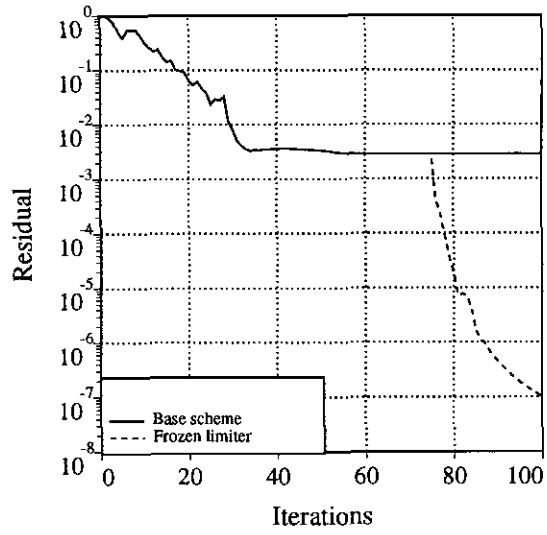

FIG. 1. Convergence histories obtained using the implicit scheme with the base scheme and with the limiter frozen after 75 iterations.

We use the spatial discretization of [4] and use an implicit scheme similar to that used by Venkatakrishnan and Mavriplis [7] for temporal discretization. A sparse linear system arises at each time step from an approximate linearization of the nonlinear problem. This sparse linear system is solved by using the Generalized Minimal Residual (GMRES) algorithm [8] with incomplete Lower Upper (LU) factorization as the preconditioner. Since the implicit side is only discretized to first-order accuracy, it does not involve the limiter. An option exists to use an explicit scheme, for which a four-stage Runge–Kutta scheme is chosen.

Figure 1 shows the convergence history for supersonic flow ($M_\infty = 2$) over an NACA0012 airfoil with an implicit scheme. It is a plot of the L_2 norm of the density residual against the number of iterations. The unstructured triangular mesh used to compute the flow has 4224 grid points. It is seen that the convergence stalls after only two orders of magnitude reduction in the residual. Even though the residual has not converged, the solution obtained is quite good and is devoid of spatial oscillations. Figure 2 shows the Mach contours using the base scheme. The problem for this lack of convergence is that the limiter function ϕ, which modulates the solution gradient and

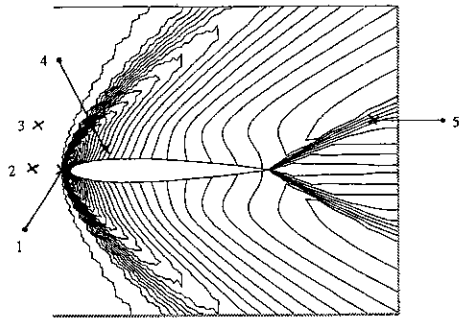

FIG. 2. Mach contours obtained with the base scheme.

which varies between 0 and 1, does not settle down. Figures 3 and 4 show the behavior of the limiter in the last 10 iterations at several points in the field indicated in Fig. 2. It may be observed that the limiter oscillates at the shock (point 1) with a small amplitude, and is fairly random in the freestream (points 2 and 3). Elsewhere in the flow field (points 4 and 5), where the gradient is nonzero, the limiter function is identically equal to 1. Thus, in these regions the limiter has converged. In the near-constant freestream regions, on the other hand, the limiter does not need to be active, but it apparently is. The limiter is thus reacting to machine-level noise. While this has almost no impact on the solution, it inhibits convergence to steady state.

Since the flipping of the limiter is the problem, freezing the limiter is one possible solution. Figure 1 also shows the convergence history with the implicit scheme when the limiter is frozen after 75 iterations. The convergence improves markedly. More generally, it is possible to freeze the limiter once some global quantity, such as the lift coefficient, is converged. Unfortunately, this approach does not always work. As an example, the convergence histories for a transonic flow problem with the explicit scheme are presented in Fig. 5. The flow conditions are $M_\infty = 0.8$, $\alpha = 1.25°$. It is observed that even after the

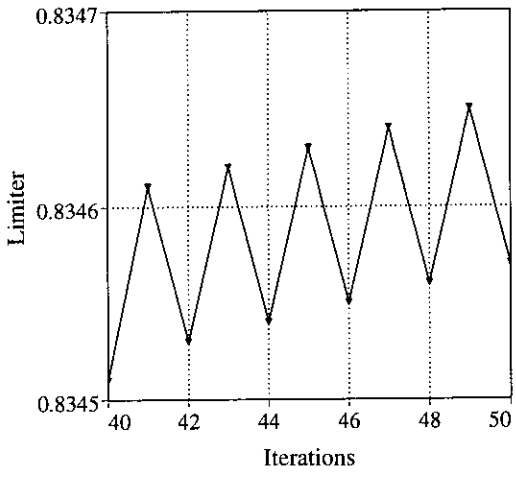

FIG. 3. The behavior of the limiter at the shock (point 1 in Fig. 2).

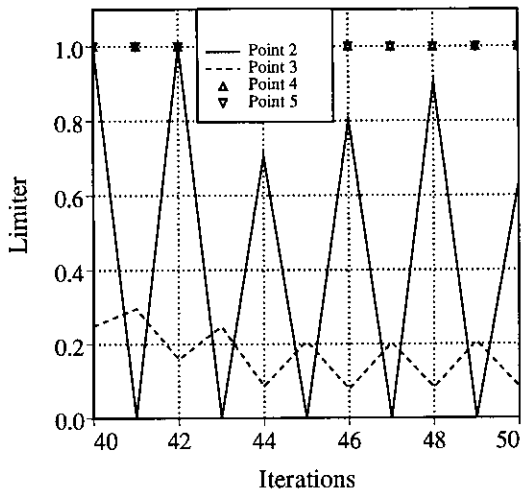

FIG. 4. The behavior of the limiter at several points indicated in Fig. 2.

limiter is frozen after 500 iterations the convergence does not improve. However, freezing the limiter did improve the convergence of the explicit scheme for the supersonic problem as well as that of the implicit scheme for the transonic problem. Thus the effectiveness of the technique of freezing the limiter is highly problem-dependent.

What is desirable is a limiter that is not active in the freestream regions. However, the transition from the limiting to the nonlimiting situation should be smooth. Only then is the convergence expected to improve.

3. THE BASE SCHEME

The scheme of Barth and Jespersen [4] will be considered as the base scheme. The key development in [4] is a multi-

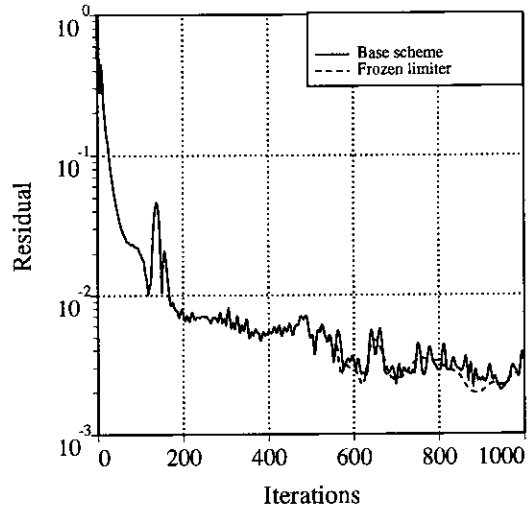

FIG. 5. Convergence histories obtained using the explicit scheme with the base scheme and with the limiter frozen after 500 iterations for the transonic flow problem.

dimensional limiter that is applicable to unstructured grids in order to satisfy monotonicity. The basic idea is to define a gradient and then modulate the gradient to satisfy monotonicity. Much work has been done in one dimension on this topic, starting with the pioneering work of Van Leer [9, 10]. A thorough discussion on slope-limiter methods may be found in the text by Leveque [11].

For the purposes of illustration, the multi-dimensional base scheme of Barth and Jespersen is outlined in one dimension. Consider a distribution of cell-averaged quantities u_i, $i = 1, ..., n$, on a uniform grid with spacing Δx. x_i is the coordinate of the centroid for cell i defined by the interval $[x_{i-1/2}, x_{i+1/2}]$. Since the distinction between cell-averaged and pointwise values at the centroid of the cell is of no consequence when dealing with second-order accurate schemes, the u_i's can also be interpreted as the pointwise values at the x_i's. The reconstructed distribution $U_i(x)$ within cell i is

$$U_i(x) = u_i + \Phi_i \nabla u_i \cdot (x - x_i), \qquad \Phi_i \in [0, 1]. \tag{2}$$

In this formula, the vector ∇u_i is the best estimate of the solution gradient in cell i computed from surrounding cell-averaged values and x is the coordinate at the point of interest. In one dimension, this gradient is taken in [4] to be a central difference approximation. The key idea in their paper is to find the largest possible Φ_i while invoking the monotonicity principle that the values of the linearly reconstructed function within cell i be bounded by the maximum and minimum of the neighboring cells (including cell i). That is, if $u_i^{\max} = \max(u_{i-1}, u_i, u_{i+1})$ and $u_i^{\min} = \min(u_{i-1}, u_i, u_{i+1})$ then they require that

$$u_i^{\min} \le U(x) \le u_i^{\max}. \tag{3}$$

This monotonicity condition coincides with that of Van Leer [9] in one dimension and that of Spekreijse [12] for structured grids in multi-dimensions. The value of Φ_i that satisfies Eq. (3) is given by

$$\Phi_i = \min(\Phi_{i+1/2}, \Phi_{i-1/2}), \tag{4}$$

where

$$\Phi_{i+1/2} = \begin{cases} \min\left(1, \dfrac{u_i^{\max} - u_i}{U(x_{i+1/2}) - u_i}\right), & \text{if } U(x_{i+1/2}) - u_i > 0 \\ \min\left(1, \dfrac{u_i^{\min} - u_i}{U(x_{i+1/2}) - u_i}\right), & \text{if } U(x_{i+1/2}) - u_i < 0 \\ 1 & \text{if } U(x_{i+1/2}) - u_i = 0. \end{cases} \tag{5}$$

$U(x_{i+1/2})$ in Eq. (5) is determined by using Eq. (2) with $\Phi \equiv 1$. $\Phi_{i-1/2}$ is obtained by replacing $i + 1/2$ with $i - 1/2$ in Eq. (5). The reconstructed value $U_{i+1/2}^L$ to the left of the interface $i + 1/2$, which is determined from the reconstruction in cell i, is then

$$U_{i+1/2}^L = u_i + \left(\frac{u_{i+1} - u_{i-1}}{2\Delta x}\right)\left(\frac{\Delta x}{2}\right)\Phi_i, \tag{6}$$

where the term $(u_{i+1} - u_{i-1})/2\Delta x$ is the central difference approximation to du/dx at cell i.

It will be shown that the scheme outlined above meets the conditions required by Spekreijse [12] for obtaining monotone steady-state solutions in two dimensions. Spekreijse has also shown that the schemes that satisfy the conditions for monotonicity in two dimensions obey the TVD property [13] in one dimension. The scheme of Barth and Jespersen will be shown to be a well known scheme in one dimension. This one-dimensional analysis is presented to serve as the framework in which the new limiter will be designed, even though the limiter is itself applicable for unstructured grids in two and three dimensions.

The analysis of Spekreijse [12] is reproduced below for a two-dimensional structured grid. Consider the following conservation law in two dimensions:

$$\frac{\partial u}{\partial t} + \frac{\partial}{\partial x} f(u) + \frac{\partial}{\partial y} g(u) = 0. \tag{7}$$

A discretization of Eq. (7) on an equidistant mesh with mesh size h is given by

$$\begin{aligned} U_{i,j}^{n+1} = U_{i,j}^n + \lambda(&A_{i+1/2,j}^n (U_{i+1,j}^n - U_{i,j}^n) \\ &+ B_{i,j+1/2}^n (U_{i,j+1}^n - U_{i,j}^n) + C_{i-1/2,j}^n (U_{i-1,j}^n - U_{i,j}^n) \\ &+ D_{i,j-1/2}^n (U_{i,j-1}^n - U_{i,j}^n)), \end{aligned} \tag{8}$$

where $\lambda = \Delta t/h$ and

$$\begin{aligned} A_{i+1/2,j}^n &= A(..., U_{i-1,j}^n, U_{i,j}^n, U_{i+1,j}^n, ...), \\ B_{i,j+1/2}^n &= B(..., U_{i,j-1,}^n, U_{i,j}^n, U_{i,j+1}^n, ...), \\ C_{i-1/2,j}^n &= C(..., U_{i-1,j}^n, U_{i,j}^n, U_{i+1,j}^n, ...), \\ D_{i,j+1/2}^n &= D(..., U_{i,j-1,}^n, U_{i,j}^n, U_{i,j+1}^n, ...), \end{aligned}$$

A scheme is called monotone if it has positive, uniformly bounded coefficients; i.e., if

$$A_{i+1/2,j}^n, B_{i,j+1/2}^n, C_{i-1/2,j}^n, D_{i,j-1/2}^n \ge 0, \tag{9}$$

and there exists a bound $G > 0$ such that for all (i, j),

$$A_{i+1/2,j}^n, B_{i,j+1/2}^n, C_{i-1/2,j}^n, D_{i,j-1/2}^n \le G. \tag{10}$$

A solution U is called monotone if for all (i, j)

$$\min(U_{i-1,j}, U_{i+1,j}, U_{i,j-1}, U_{i,j+1}) \le U_{i,j} \le \max(U_{i-1,j}, U_{i+1,j}, U_{i,j-1}, U_{i,j+1}). \tag{11}$$

Dropping the subscripts on the coefficients A, B, C, and D for convenience, with the scheme given by Eq. (8), at steady state we have

$$U_{i,j} = \frac{AU_{i+1,j} + BU_{i,j+1} + CU_{i-1,j} + DU_{i,j-1}}{A + B + C + D}, \tag{12}$$

which meets the monotonicity requirements of Eq. (11) if the scheme obeys the conditions given by Eqs. (9) and (10). Spekreijse also shows for λ sufficiently small ($\lambda \le 1/2G$) that the scheme given by Eq. (8) is TVD in one space dimension. Given the cell-averaged values $U_{i,j}$, Spekreijse considers reconstructions of the form

$$U^L_{i+1/2,j} = U_{i,j} + \frac{1}{2}\psi(R_{i,j})(U_{i,j} - U_{i-1,j}),$$

$$U^R_{i-1/2,j} = U_{i,j} + \frac{1}{2}\psi\left(\frac{1}{R_{i,j}}\right)(U_{i,j} - U_{i+1,j}),$$

$$U^L_{i,j+1/2} = U_{i,j} + \frac{1}{2}\psi(S_{i,j})(U_{i,j} - U_{i,j-1}),$$

$$U^R_{i,j-1/2} = U_{i,j} + \frac{1}{2}\psi\left(\frac{1}{S_{i,j}}\right)(U_{i,j} - U_{i,j+1}),$$

$$R_{i,j} = \frac{U_{i+1,j} - U_{i,j}}{U_{i,j} - U_{i-1,j}},$$

$$S_{i,j} = \frac{U_{i,j+1} - U_{i,j}}{U_{i,j} - U_{i,j-1}}.$$

The main contribution of Spekreijse lies in the formulation of the conditions on the limiter function ψ[1] to obtain second-order accuracy and monotone steady-state solutions using a flux-split finite volume formulation. He has also shown that ψ has to be a piecewise linear or a nonlinear function in order to meet these conditions. He has derived the following conditions on the limiter function $\psi(R)$ to meet the positivity and boundedness conditions given by Eqs. (9) and (10). These are

$$\alpha \le \psi(r) \le M, \qquad \forall r \tag{13}$$

$$-M \le \frac{\psi(r)}{r} \le 2 + \alpha, \qquad \forall r \tag{14}$$

[1] In this section as well as in the next section, ψ will be referred to as the limiter to be consistent with Spekreijse's notation.

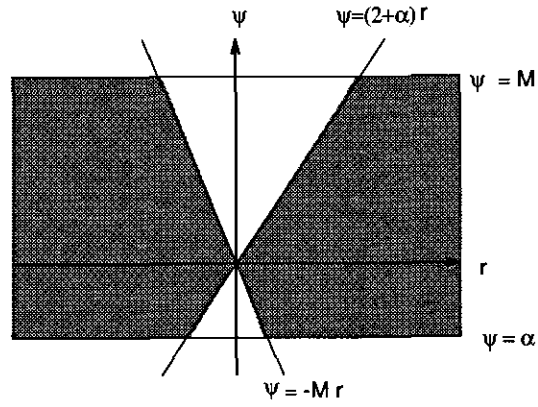

FIG. 6. Monotonicity region.

where $\alpha \in [-2, 0]$ and $M < \infty$. This monotonicity region is depicted in Fig. 6.

The conditions given by Eqs. (13) and (14) are very general and many schemes can be derived that meet these conditions. Spekreijse also shows that a spatial discretization is second order accurate away from the points where $du/dx = 0$ if $\psi(1) = 1$ and $|\psi'|$ and $|\psi''|$ are uniformly bounded.

We will now carry out an analysis of the base scheme and reformulate it in Spekreijse's framework. We will show that, depending on whether we choose central, upwind, or downwind difference approximations to the gradient at cell i, three different schemes that meet the monotonicity requirements can be derived. The scheme of Barth and Jespersen can be recast as follows:

$$U^L_{i+1/2} = u_i + \frac{1}{4}(u_{i+1} - u_{i-1})\min(\Phi_{i+1/2}, \Phi_{i-1/2}), \tag{15}$$

$$\Phi_{i+1/2} = \begin{cases} \min\left(1, \dfrac{u_i^{\max} - u_i}{((u_{i+1} - u_{i-1})/4)}\right), & \text{if } u_{i+1} > u_{i-1}, \\ \min\left(1, \dfrac{u_i^{\min} - u_i}{((u_{i+1} - u_{i-1})/4)}\right), & \text{if } u_{i+1} < u_{i-1}, \\ 1, & \text{if } u_{i+1} = u_{i-1}, \end{cases} \tag{16}$$

$$\Phi_{i+1/2} = \begin{cases} \min\left(1, \dfrac{u_i^{\max} - u_i}{((u_{i+1} - u_{i-1})/4)}\right), & \text{if } u_{i+1} < u_{i-1}, \\ \min\left(1, \dfrac{u_i^{\min} - u_i}{((u_{i+1} - u_{i-1})/4)}\right), & \text{if } u_{i+1} > u_{i-1}, \\ 1, & \text{if } u_{i+1} = u_{i-1}, \end{cases} \tag{17}$$

If u_i is bounded between u_{i-1} and u_{i+1}, $u_i^{\max}$ and $u_i^{\min}$ are given by u_{i-1} and u_{i+1} or vice versa. Then $U^L_{i+1/2}$ can be shown to be

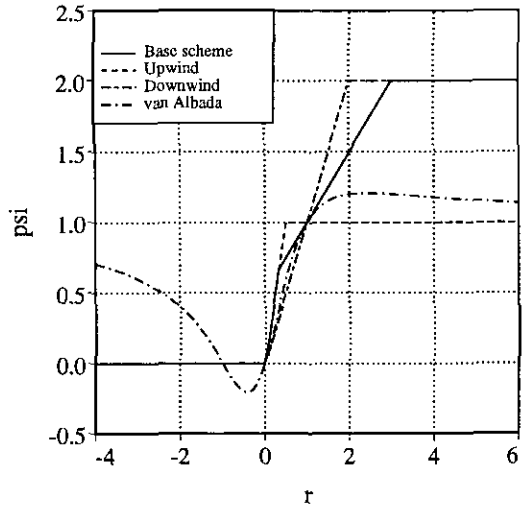

FIG. 7. Limiter functions for various schemes.

$$U^L_{i+1/2} = u_i + \frac{1}{2}\psi(r_i)(u_i - u_{i-1}), \tag{18}$$

$$\psi(r) = \frac{1}{2}(r+1)\min\left[\min\left(1, \frac{4r}{r+1}\right), \min\left(1, \frac{4}{r+1}\right)\right], \tag{19}$$

$$r_i = \frac{u_{i+1} - u_i}{u_i - u_{i-1}}. \tag{20}$$

If u_i is a maximum or a minimum, i.e., $u_i > u_{i-1}$, u_{i+1} or $u_i < u_{i-1}$, u_{i+1}, either $\Phi_{i+1/2}$ or $\Phi_{i-1/2}$ is zero while the other is positive, and hence $\psi(r) \equiv 0$, $\forall r \leq 0$. The scheme thus reduces to first order accuracy at extrema. The function $\psi(r)$ is shown in Fig. 7. It clearly satisfies the conditions of Spekreijse with $M = 2$.

In one dimension, the scheme of Barth and Jespersen is thus the Fromm scheme with the minmod limiter applied to enforce monotonicity whenever $r \leq 1/3$ or $r \geq 3$. If the central difference gradient in Eq. (6) were replaced by one-sided gradients, we obtain two more schemes that also obey the conditions of Spekreijse. These are shown in Fig. 7 as well. With the gradient approximated by the upwind approximation $(u_i - u_{i-1})/\Delta x$, the limiter function can be shown to be

$$\psi(r_i) = \min(1, 2r_i). \tag{21}$$

With the gradient approximated by the downwind approximation $(u_{i+1} - u_i)/\Delta x$, the limiter function is

$$\psi(r_i) = \min(r_i, 2). \tag{22}$$

A downwind approximation for the gradient is akin to Lax–Wendroff, whereas an upwind approximation yields the Beam–Warming scheme [14]. See the text by Leveque [11] for a discussion on this topic. For the limiters discussed above, $\psi(r) \equiv 0$, $\forall r \leq 0$. Finally, Fig. 7 also shows the van Albada limiter which is

$$\psi(r) = \frac{r^2 + r}{r^2 + 1}. \tag{23}$$

Note that all the schemes discussed above are second-order accurate away from points where $du/dx = 0$.

Many other limiters have been surveyed by Sweby [16] and these are used primarily in the context of structured grids.

4. ACCURACY WITH LIMITERS

The schemes with the limiters should exhibit second-order accuracy in all norms if the initial profile possesses no extrema [13]. However, most profiles that are advected have finite support and hence have at least one extremum. The schemes without limiters exhibit uniform second-order accuracy in all the norms but produce nonmonotone profiles, whereas the schemes with limiters exhibit second-order accuracy only in the L_1 norm. The reason for the drop in the order of accuracy in the other norms is due just to the clipping of the extrema. As discussed below, the schemes can be easily modified to obtain second-order accuracy in all norms.

In the following, we will first show that the scheme that uses the van Albada limiter can be modified to restore second-order accuracy. Modifications to the base scheme, for use in unstructured grids, will be devised based on the insight gained from modifying the van Albada limiter. The modification to the limiter is the one proposed by van Albada *et al.* [6] to avoid clipping smooth extrema. The scheme with van Albada limiter is given by

$$\begin{aligned} u^L_{i+1/2} &= u_i + \frac{1}{2}\left(\frac{r^2 + r}{r^2 + 1}\right)(u_i - u_{i-1}), \\ r &= \frac{\Delta_+}{\Delta_-}, \\ \Delta_+ &= u_{i+1} - u_i, \\ \Delta_- &= u_i - u_{i-1}. \end{aligned} \tag{24}$$

The modified van Albada scheme is

$$u^L_{i+1/2} = u_i + \frac{1}{2}\frac{(\Delta_+^2 + \varepsilon^2)\Delta_- + (\Delta_-^2 + \varepsilon^2)\Delta_+}{\Delta_+^2 + \Delta_-^2 + 2\varepsilon^2}. \tag{25}$$

ε^2 is made proportional to $(\Delta x)^3$. In the smooth regions of the solution, $(\Delta_+, \Delta_-) \sim \Delta x$. At the extremum as well as in the near-constant regions, ε^2 dominates Δ_+^2, Δ_-^2 and we recover the $\kappa = 0$ scheme without limiting. We set $\varepsilon^2 = (K\,\Delta x)^3$ where K is a constant. If K is set to zero, the original scheme is recovered. A large value of K implies no limiting at all and

the $\kappa = 0$ scheme is obtained. We have verified that for a fixed value of K, second-order accuracy is approached with such an approach. However, the advected distribution is not monotone. This is because of the scheme reverting to the unlimited scheme in the near-constant regions. If in addition, it is ensured that such a modification is made only near true extrema, we obtain a globally second-order accurate scheme (in all norms) that also produces monotone profiles.

The modification to the van Albada limiter immediately suggests a modification for the limiter of Barth and Jespersen. Whereas the modification to the van Albada limiter is smooth in suppressing the action of the limiter at extrema and in the near-constant regions, the proposed modification is not smooth. This modification eliminates the action of the limiter whenever the absolute values of the numerator and the denominator in Eqs. (5) are less than a threshold, which is set equal to $(K\Delta)^{1.5}$. This modification will be referred to as *conditional threshold*. Once again the scheme is globally second-order accurate in all norms, but the solution is not monotone. Second-order accurate monotone solutions can again be obtained by ensuring that this switch to the unlimited scheme takes place only at true extrema.

Another approach to restoring global second-order accuracy has been pursued by Shu [15]. By relaxing the TVD requirement and allowing the total variation to increase with an upper bound, he has derived a class of schemes termed TVB (total-variation-bounded) schemes. The min-mod function

$$m(a1, a2) = \begin{cases} s.\min(|a_1|, |a_2|), & \text{if } \operatorname{sign}(a_1) = \operatorname{sign}(a_2) = s, \\ 0, & \text{otherwise,} \end{cases} \tag{26}$$

is replaced by the modified function

$$mc(a1, a2) = m(a_1, a_2 + M\,\Delta x^2 \operatorname{sign}(a_1)). \tag{27}$$

Shu has been able to prove rigorously that an upwind scheme using this limiter is strictly TVB. Even though such a rigorous proof is not available for van Albada limiter modification, our experiments in one dimension seem to indicate that the total variation is bounded.

The nonsmooth modification given above for the base scheme as well as Shu's modification, while restoring second-order accuracy for the advection problem, is unsuitable for obtaining converged steady-state solutions in multi-dimensions. As will be demonstrated in the next section, convergence stalls with the base scheme after a few orders of magnitude reduction in the residual when marching to steady state. When solving nonlinear problems to steady state, the smoothness of the limiter is an important consideration. For example, if a Newton's method is used to solve the nonlinear system of equations, a differentiable limiter is required. In the case of other iterative methods, there is experimental evidence to suggest that differentiability of limiters is a desirable property. The conditional threshold modification only makes matters worse in this respect. The modified van Albada limiter, on the other hand, transitions smoothly to the unlimited scheme in the near-constant regions and has been shown to aid in the convergence to steady state [5]. It is desirable to devise a modification to the base scheme that handles the freestream region likewise in a smooth manner. Such a modification is expected to improve convergence when computing steady-state solutions on unstructured grids.

5. THE NEW LIMITER

The base scheme in the form given by Eqs. (2)–(5) needs to be modified. It is this form, given by Barth and Jespersen, that is suitable for unstructured grids. Therefore, we seek an approximation $\phi(y)$ to the function $\min(1, y)$. Equation (19) then becomes

$$\psi(r) = \frac{1}{2}(r+1)\min\left[\phi\left(\frac{4r}{r+1}\right), \phi\left(\frac{4}{r+1}\right)\right]. \tag{28}$$

It is imperative that this new function $\psi(r)$ be completely contained under the original curve shown in Fig. 7 for the base scheme. Otherwise, the monotonicity requirements are violated and oscillations are amplified. Since a modification similar to that for the van Albada limiter is desired, $\phi(y)$ is taken to be a ratio of second-degree polynomials. The condition $\psi(1) = 1$ for second-order accuracy implies $\phi(2) = 1$. In addition, we stipulate that the curve for $\phi(y)$ be contained under the curve $z(y) = y$. This condition is required in order for $\psi(r)$ to be contained under the curve for the original limiter. It is further required that $\phi(\infty) = 1$ and $\phi(0) = 0$. The function ϕ satisfying these conditions is given by

$$\phi(y) = \frac{y^2 + 2y}{y^2 + y + 2}. \tag{29}$$

The functions $\phi(y)$ and $\min(1, y)$ intersect at $y = 2$ and $\phi(y) > 1, \forall y > 2$. However, this is of no consequence for the function $\psi(r)$ which is given by

$$\psi(r) = \frac{1}{2}(r+1)\min\left[\frac{4r(3r+1)}{11r^2 + 4r + 1}, \frac{4(r+3)}{r^2 + 4r + 11}\right]. \tag{30}$$

The new limiter and the old limiter are displayed in Fig. 8. The curve for the new limiter is completely contained under that for the original limiter. The new limiter does have a slope discontinuity at $r = 1$. Also shown in Fig. 8 is the limiter due to Van Leer [10] (which does not have a slope discontinuity at $r = 1$):

$$\psi(r) = \frac{r + |r|}{r + 1}. \tag{31}$$

The new limiter is quite close to the van Leer limiter. The functional form of the new limiter is different and makes the limiter amenable to the modification described below. By simply replacing the min(1, y) function in the multi-dimensional limiter by the function $\phi(y)$, the new limiter may be applied to unstructured grids in a straightforward manner. On the other hand, applying the van Leer limiter in an unstructured grid context is far more involved, because it is not clear as to how the two successive gradients should be defined in order to satisfy monotonicity principles in multiple dimensions.

The new limiter can easily be modified to transition smoothly to the unlimited scheme in the near-constant regions of the solution. In the original scheme given by Eqs. (2)–(5), the key step is the determination of the function $\Phi_{i+1/2}$. With the function min(1, y) approximated by $\phi(y)$, Eq. (5) becomes

$$\Phi_{i+1/2} = \begin{cases} \phi\left(\dfrac{u_i^{\max} - u_i}{U(x_{i+1/2}) - u_i}\right), & \text{if } U(x_{i+1/2}) - u_i > 0 \\ \phi\left(\dfrac{u_i^{\min} - u_i}{U(x_{i+1/2}) - u_i}\right), & \text{if } U(x_{i+1/2}) - u_i < 0 \\ 1, & \text{if } U(x_{i+1/2}) - u_i = 0. \end{cases} \tag{32}$$

Without loss of generality assume $U(x_{i+1/2}) - u_i > 0$ since the other cases can be handled in a similar manner. Letting $\Delta_- = U(x_{i+1/2}) - u_i$ and $\Delta_+ = u_i^{\max} - u_i$,

$$\Phi_{i+1/2} = \phi\left(\frac{\Delta_+}{\Delta_-}\right),$$

$$= \left(\frac{1}{\Delta_-}\right)\Delta_-\phi\left(\frac{\Delta_+}{\Delta_-}\right).$$

Akin to the modification for the van Albada limiter, the term $\Delta_-\phi(\Delta_+/\Delta_-)$ is modified. With $\phi(y)$ defined by Eq. (29), $\Phi_{i+1/2}$ becomes

$$\Phi_{i+1/2} = \frac{1}{\Delta_-}\left[\frac{(\Delta_+^2 + \varepsilon^2)\Delta_- + 2\Delta_-^2\Delta_+}{\Delta_+^2 + 2\Delta_-^2 + \Delta_-\Delta_+ + \varepsilon^2}\right]. \tag{33}$$

Once again ε^2 is taken to be $(K\,\Delta x)^3$. In the smooth regions of the solution $\Delta_-, \Delta_+ \sim \Delta x$. In the near-constant regions ε^2 dominates Δ_-^2, Δ_+^2, and $\Delta_-\Delta_+$, and $\Phi_{i+1/2}$ reduces to 1. Thus the scheme reverts to the scheme without limiting in the near-constant regions. As a practical matter, to avoid division by a very small value of Δ_- in Eq. (33), Δ_- should be replaced by $\text{Sign}(\Delta_-)(|\Delta_-| + \omega)$ where ω is taken to be 10^{-12} for 64-bit arithmetic computations. The new limiter is more diffusive than the original limiter and this fact is reflected in Fig. 8. Whereas the original limiter allows twice the upwind slope to be used for $r \geq 3$, the new limiter only asymptotes to this value.

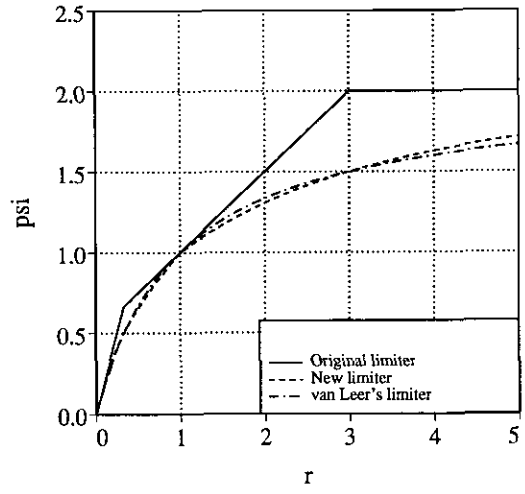

FIG. 8. The new limiter, the old limiter, and the van Leer limiter.

Second-order accuracy in all norms is obtained by using the modified limiter but the resulting solutions are not monotone. However, by ensuring that the modification is only made at the true extrema, we once again realize a scheme that is second-order accurate in all norms and that produces monotone profiles.

6. LIMITERS AND CONVERGENCE

Supersonic flow over an NACA0012 airfoil at a freestream Mach number of 2 and 0° angle of attack is revisited. The mesh has 4224 vertices and the far field boundary is located 50 chords away from the airfoil. A limiter is essential to compute this flow; in its absence, the solution procedure becomes unstable after a few iterations. The nondimensional time step is allowed to vary between 1 and 100 inversely proportional to the L_2 norm of the residual. Figure 9 shows the convergence histories with the scheme of Barth and Jespersen and with a first-order accurate scheme. While the first-order accurate scheme converges rapidly, the second-order accurate scheme stalls after about two orders of magnitude reduction in the residual.

The new limiter given by Eq. (33) is expected to ameliorate convergence. On nonuniform triangular grids we take $\varepsilon^2 = (K\overline{\Delta})^3$ where $\overline{\Delta}$ is an average grid size and K is a constant. $\overline{\Delta}$ is taken to be the length of an equilateral triangle in an equivalent uniform triangulation with the same number of triangles covering the same physical area as the original grid. K is a parameter and signifies a threshold. Oscillations below this threshold are allowed to exist in the solution and are not dealt with by the limiter. A value of zero implies that the limiter is active even in the near-constant regions, whereas a very high value for K implies effectively no limiting at all. While setting K to be a large value is acceptable for subcritical flows, for

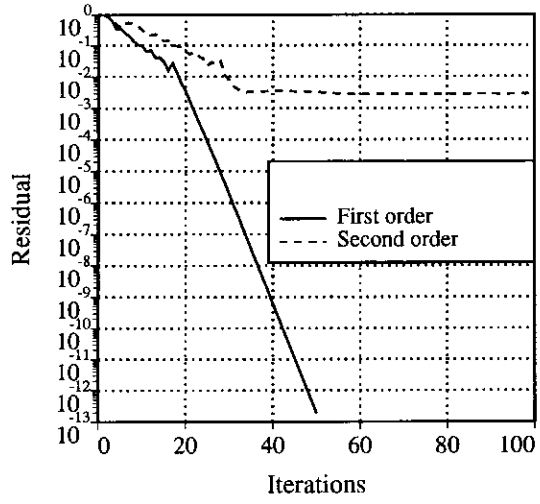

FIG. 9. Convergence histories obtained with the first-order and the second-order accurate schemes for the supersonic flow case.

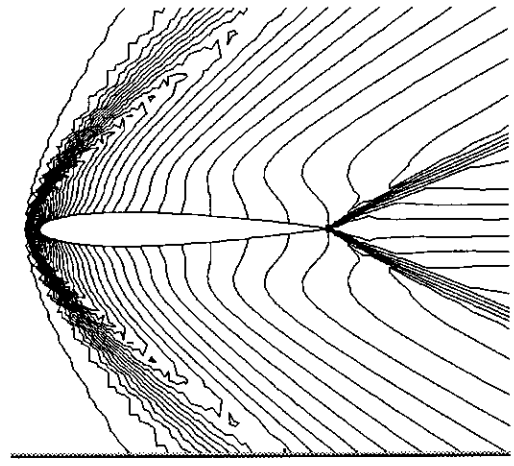

FIG. 11. Mach contours obtained with the modified scheme.

flows with discontinuities this will cause the solution procedure to become unstable. Thus, for solutions with discontinuities, as K is increased from 0, the convergence of the scheme will improve until the solution procedure possibly becomes unstable for large values of K. Figure 10 shows the convergence histories obtained with the modified scheme for the supersonic flow case with K set to 0.1 and 0.3. Note the improvement in convergence as the value of K is increased. Figure 11 shows the Mach contours of the steady-state solution with the K set to 0.3. The islands in Fig. 11 indicate oscillations of small amplitude that are allowed to exist in the solution. Figure 10 also shows the convergence history obtained with the base scheme with the limiter modified using conditional threshold. Here ε is set to $(0.3\overline{\Delta})^{1.5}$. Convergence worsens in comparison with the base scheme since the modification to the limiter is not smooth.

To demonstrate that the phenomenon of convergence stall is independent of the time discretization, an explicit scheme is also used solve the supersonic flow problem. A four-stage Runge–Kutta scheme is used for this purpose with a CFL number of 1.2. Figure 12 shows the convergence histories obtained with the base scheme and with the new limiter. Once again convergence stalls after about four orders of magnitude reduction in the residual with the original limiter, whereas it is markedly improved with the new limiter ($K = 0.3$). Also shown in Fig. 12 is the convergence history with the original limiter modified using a conditional threshold, with ε set to $(0.3\overline{\Delta})^{1.5}$. Convergence deteriorates again in comparison with the base scheme. It may also come as a surprise that the original scheme achieves nearly four orders of reduction in the residual

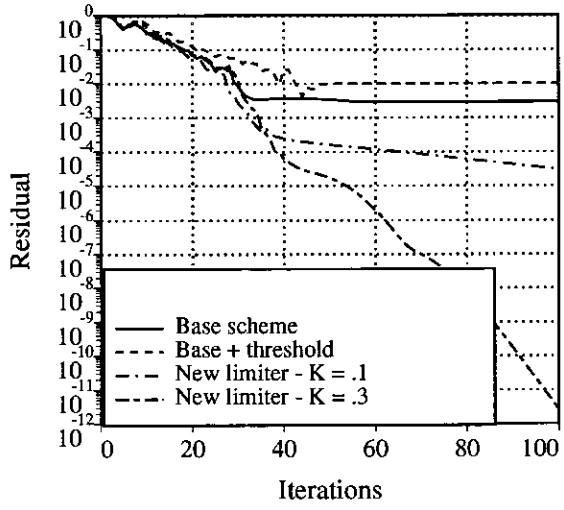

FIG. 10. Convergence histories with the new limiter and the old limiter with conditional threshold modification.

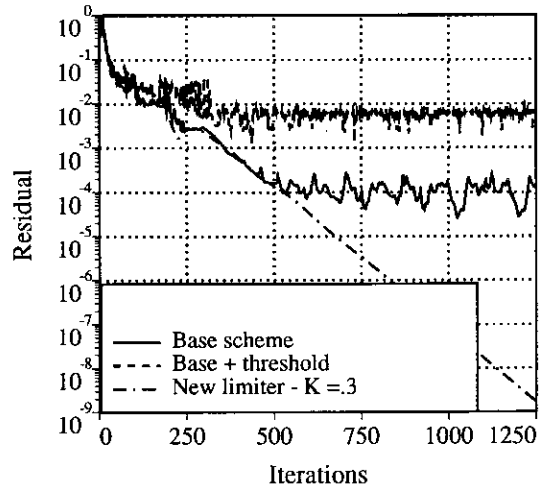

FIG. 12. Convergence histories with the explicit scheme.

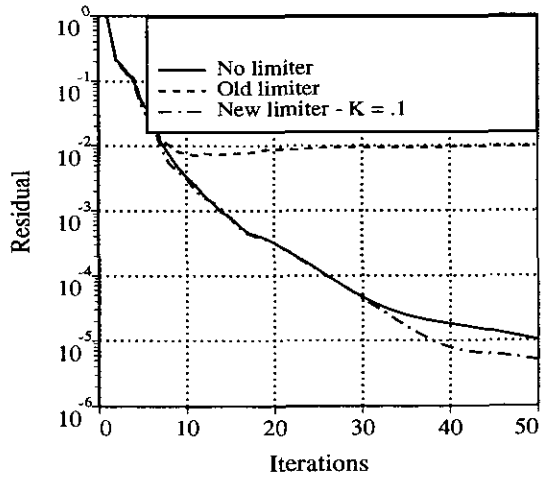

FIG. 13. Convergence histories for the subcritical flow case.

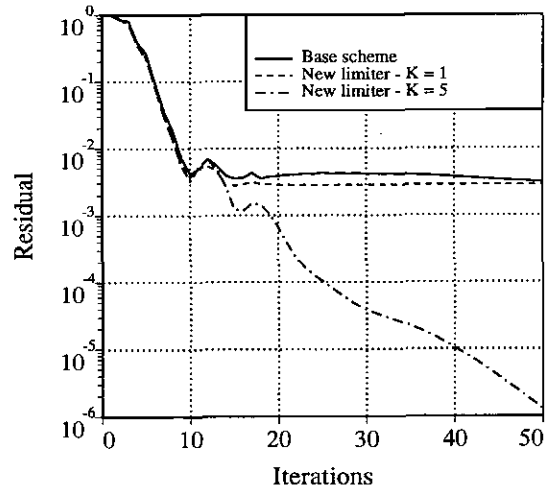

FIG. 14. Convergence histories for transonic flow over an NACA0012 airfoil.

with the explicit scheme, whereas it stalled after only about two orders with the implicit scheme.

The phenomenon of convergence slowdown also occurs in subcritical flows when limiters are used. Here limiters are not essential to obtain solutions and the effects of the limiters, if used, should be benign. We consider flow over a four-element airfoil in landing configuration at a freestream Mach number of 0.2 and angle of attack of 5°. The triangular mesh has 6019 vertices. Figure 13 shows the convergence histories without the limiter, with the original limiter, and with the modified limiter. Convergence stalls with the original limiter, whereas convergence with the new limiter is comparable to the scheme without limiting. Convergence is only shown with the parameter K set to 0.1. Convergence with $K = 0.3$ is identical to that without limiting.

Rather than use a global average grid size to base the threshold for turning off the limiter, it is advisable to use the local grid size, especially when dealing with highly nonuniform grids. At grid point i, ε_i^2 is taken to be $(K\overline{\Delta}_i)^3$, where $\overline{\Delta}_i$ is the local grid size. Since a cell-vortex scheme is used, the control volume is a polygon made up of segments of the medians of the triangles. This control volume can be approximated as a circle and $\overline{\Delta}_i$ can be taken to be the diameter of this circle. Results are presented for the case of transonic flow over an NACA0012 airfoil at a freestream Mach number of 0.8 and angle of attack of 1.25° using this approach. Figure 14 shows the convergence histories and Fig. 15 displays the surface pressure profiles obtained with the base scheme and with the new limiter for two values of K.

These figures clearly show the tradeoff between convergence and obtaining monotone steady-state solutions. With $K = 1$, the convergence hardly improves and the pressure profile matches that of the base scheme. With $K = 5$, convergence improves dramatically, but the surface pressure on either side of the shock on the upper surface shows a discrepancy. The weaker shock on the lower surface on the other hand exhibits no such discrepancy. The reason for the discrepancy near the shock on the suction side is that the flow is nearly constant upstream of the shock and the modified limiter reverts to the scheme without limiting. It may be possible to eliminate the undesirable side effects near the stronger shock by using a shock sensor and ensuring that the limiter is not turned off. Figure 16 shows the lift histories with the three schemes during the latter iterations. The base scheme exhibits an odd-even mode as does the new limiter with $K = 1$, whereas the new limiter with $K = 5$ converges monotonically. However, even with the base scheme the variation is only in the fourth decimal place. Thus, when using the base scheme, it is possible to declare convergence once the mean lift coefficient no longer varies, especially since the variations about the mean are small. Another observation that can be made from Fig. 16 is that the

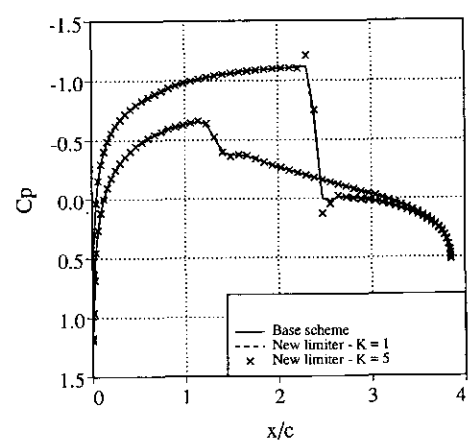

FIG. 15. Surface pressure profiles for transonic flow over an NACA0012 airfoil.

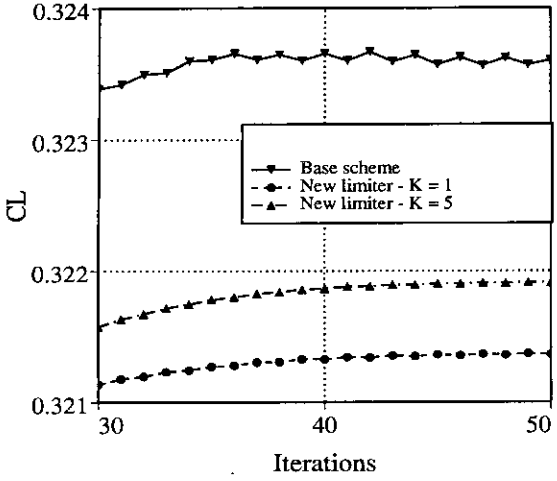

FIG. 16. Lift coefficient histories for the transonic flow case.

lift coefficient with the base scheme is higher, which is due to the fact that the new limiter is more diffusive than the original limiter.

With the local thresholding, the constant K had to be increased to 100 in order to obtain convergence comparable to the scheme without limiting for the subcritical flow over the four-element airfoil discussed earlier. Otherwise, all the trends observed when using a global threshold hold true when using a local threshold. One possible way to determine the value of K for use in supercritical flows is to solve a subcritical problem on the same grid and find the smallest value of K that yields convergence comparable to the scheme without limiting.

7. CONCLUSIONS

It is shown in this paper that the limiters currently in use with upwind schemes on unstructured grids inhibit convergence to steady state of the two-dimensional Euler equations. The reason for this is the way the limiters handle the near-constant regions of the solution. Modifications are proposed to the limiter which solves this problem at the expense of monotonicity. While the original scheme fails to converge for supersonic flow computations on unstructured grids, the modified scheme is shown to converge quite well. The improvement in convergence comes at a cost; the solution exhibits deviations from the monotone solution near strong shocks.

ACKNOWLEDGMENTS

The author thanks the NAS Applied Research Branch at the NASA Ames Research Center for supporting this project. The author also thanks Marsha Berger of the Courant Institute of Mathematical Sciences for numerous motivating discussions on limiters and Tim Barth of NASA Ames research center for providing the code for the explicit scheme. The author thanks the reviewers for their comments.

REFERENCES

1. P. L. Roe. *J. Comput. Phys.* **43**(7), 357 (1981).
2. V. Venkatakrishnan and T. J. Barth, Application of direct solvers to unstructured meshes for the Euler and Navier–Stokes equations using upwind schemes, in *27th AIAA Aerospace Sciences Meeting, Reno, NV, 1989*, Paper AIAA 89-0364.
3. J. T. Batina, *AIAA J.* **28**(8), 1381 (1990).
4. T. J. Barth and D. Jespersen, The design and application of upwind schemes on unstructured meshes, in *27th AIAA Aerospace Sciences Meeting, Reno, NV, 1989*, Paper AIAA 89-0366.
5. V. Venkatakrishnan, *AIAA J.* **29**(7), 1092 (1991).
6. G. D. van Albada, B. van Leer, and W. W. Roberts, *Astron. and Astrophys.* **108,** 76 (1982).
7. V. Venkatakrishnan and D. J. Mavriplis, *J. Comput. Phys.* **105**(1), 83 (1993).
8. Y. Saad and M. H. Schultz, *SIAM J. Sci. Statist. Comput.* **7**(3), 856 (1986).
9. B. van Leer, *J. Comput. Phys.* **14,** 361 (1974).
10. B. van Leer, *J. Comput. Phys.* **11,** 276 (1977).
11. R. J. Leveque, *Numerical Methods for Conservation Laws*, 2nd ed. (Birkhauser, Basel, 1992).
12. S. P. Spekreijse, *Math. Comput.* **49**(179), 135 (1987).
13. A. Harten, *J. Comput. Phys.* **49,** 357 (1983).
14. R. Beam and R. F. Warming, *J. Comput. Phys.* **22,** 87 (1976).
15. C. Shu, *Math. Comput.* **49**(179), 105 (1987).
16. P. K. Sweby, *SIAM J. Numer. Anal.* **21**(5), 995 (1984).